Solid lubrication with MoS_2-Ti-C films for high-vacuum applications in a nuclear fusion device

Shanshuang SHI[1, 2], Huapeng WU[1], Yuntao SONG[2], Heikii HANDROOS[1]

Laboratory of Intelligent Machines, Lappeenranta University of Technology, Finland

Institute of Plasma Physics, Chinese Academy of Sciences, Hefei, China

Corresponding author: Shanshuang SHI

shiss@ipp.ac.cn

Abstract:

Purpose: EAST is a tokamak fusion device running in ultra-high vacuum condition. To avoid polluting the inner vessel environment, solid lubrication has been applied on the surface of bearings and gears which exposed to the vacuum. **Design/methodology/approach:** anti-friction MoS2 coatings penetrating with different atoms have been developed by multi-target magnetron sputtering deposition technique. This paper presents the comparative testing of tribological properties for three kinds of MoS2-based coating layers.

Findings: based on the test results, MoS2-Ti-C coating films are supposed to be the final selection due to the better performance of friction coefficient and lubrication longevity.

Originality/value: finally, the detailed information has been characterized for the hybrid coatings which can provide some references for applications of solid lubrications in similar condition of high vacuum and temperature.

***Keywords*:** Solid lubrication; Adhesive wear; Coating; Vacuum; Lubrication performance

1. Introduction

Experimental Advanced Superconducting Tokamak (EAST) is the first fully superconducting tokamak fusion device, which is built in China [1-3]. The former records of EAST physical experiments indicate a fact that more than 30% of shutdown and maintenance are caused by the damages of small pieces inside the vacuum vessel (VV) due to huge heat flux [4, 5]. Fig 1 shows the EAST tokamak device and its vacuum vessel with a pressure of 10^{-5} Pa.

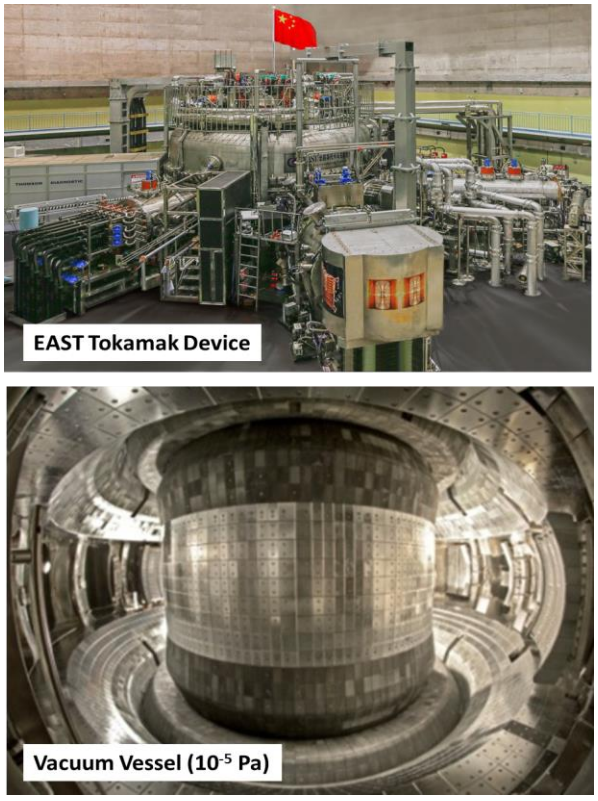

Fig. 1. EAST tokamak device and its vacuum vessel with a pressure of 10^{-5} Pa.

To increase the effective running time, it will be more efficient to repair damaged pieces without breaking the vacuum environment. EAST Articulated Maintenance Arm (EAMA) is a series robot system, seen in Fig.2, which is developed for the purpose of remote maintenance in EAST vacuum vessel during plasma pulses [6, 7]. The operational conditions for EAMA robot can be summarized as high temperature (~80 ºC), high vacuum (~10^{-5} Pa) and high loads (~1000Nm), in which case, perfect lubrication for motion joints should be guaranteed.

Fig. 2. The conceptual design of EAMA robot arms and its end effector

For the whole robot mechanism, hundreds of bearings and gears are assembled inside the articulated joints to guarantee the robot moving smoothly. All high-speed ones (motors, gears, etc.) which should be lubricated very well, are sealed in boxes to prevent polluting vacuum condition, in which case high temperature grease can be used. Meanwhile, some low-speed components (joint bearings and bushes) are considered to use coating films as solid lubrication, seen in Fig. 3.

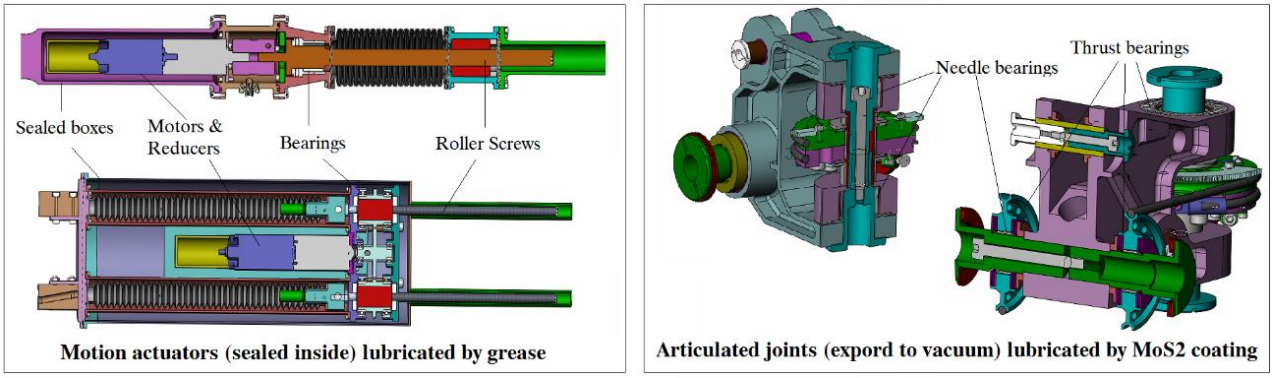

Fig. 3. The lubrication selections for different components in EAMA robot

Considering solid lubrication in EAMA robot, some requirements can be summarized as below:

1) Good reliability in vacuum (10^{-4}~10^{-5} Pa) and high temperature (~80℃);
2) To stand high compression forces up to 30 kN;
3) Low friction coefficient (~0.1) to allow smoothly moving;
4) Thin film thickness to guarantee the assembly accuracy of bearings.

Solid lubricant films based on MoS_2 are widely used in vacuum conditions [8-10]. However, when exposed to atmosphere with a certain humidity, MoS_2 is highly vulnerable to oxidation [11-13]. Moreover, for high precision applications, the thin films deposited by sputtering techniques will lead poor adhesion and low lifetime because of the ionization limitation of process [14]. To improve the performance of solid lubrication, this paper presents a study work on composite coating films based on MoS_2 using multi-target magnetron sputtering deposition technique. Scanning Electron Microscopy (SEM) images and X-ray Diffraction (XRD) patterns of different composite films have been obtained. MoS_2-Ti-C films are supposed to be the final selection due to the better tribological properties. Finally, the

detailed information has been characterized for the composite coating which can provide some reference for applications of solid lubrications in similar condition of high vacuum and temperature.

2. Composite coating films based on MoS_2

Sputtering deposition for composite coating films has been performed on Bearing Steel GCr15 with a single chamber magnetron sputtering system JGP-450, which can provide a base pressure of high vacuum at 6.67×10^{-5} Pa after baking and degassing. The sputtering system contains three magnetron targets, where MoS_2, Ti and C target plates were respectively mounted on, shown in Fig. 4.

Fig. 4. The Single Chamber Magnetron Sputtering System and Multi targets

Three different coating films（MoS_2, MoS_2-Ti, MoS_2-Ti-C）have been deposited to find a better one forbearing lubricating in EAMA robot. The detailed deposition parameters are given in Table 1.

Table. 1. Deposition parameters of coating films

Target	MoS_2, MoS_2-Ti, MoS_2-Ti-C
Chamber pressure	1.1×10^{-4} Pa
Substrate material	GCr15
Substrate temperature	200 ℃
Substrate negative bias	-200 V
Magnetron current	0.5~1.0 A

Coating time	60 min

3. Microstructure evaluation

3.1 Morphology of MoS2-based films

The surface and cross-section SEM images of pure MoS_2 and composite films are illustrated in Fig. 5, where 1 μm is treated as the standard film thickness for comparison.

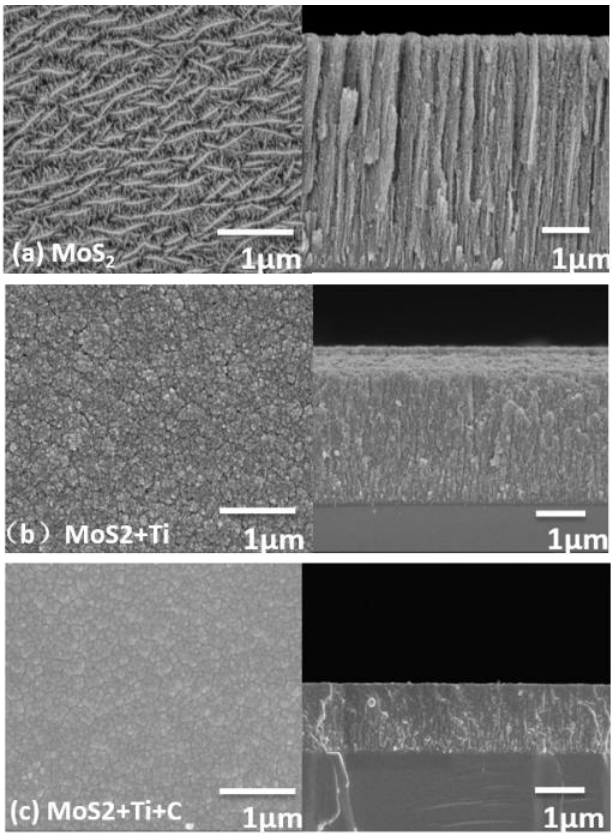

Fig. 5. The surface and cross-section SEM images of MoS2-based films

Similar to the images in other related work [13, 14], the pure MoS_2 films shown a worm-like surface structure with different size of aggregates. When combining with Ti atoms, the nanocrystals of composite films were obviously refined. However, some small gaps can still be found. After further penetrating with C atoms, the mound-like protrusions and film particles became finer, smoother and more compact, which indicated better hardness and wear resistance.

3.2 Microstructure analysis

Fig. 6 shows the patterns of the three different films by RINT2400 type of X-ray diffraction (XRD).

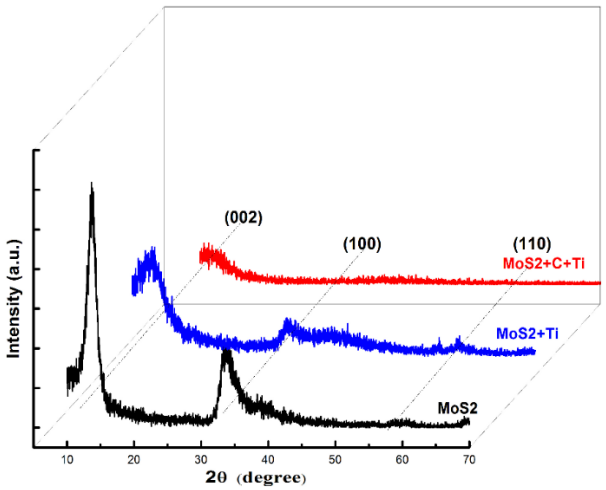

Fig.6. The XRD patterns of pure MoS_2 and composite films (Specific testing conditions: Cu target, the scanning speed of 10 °/ min, step width 0.02 °, voltage 40 kV, current 150 mA, scan range: 10 °~ 70 °)

By Comparing the XRD patterns, some facts can be indicated and summarized as bellow:

1) For pure films, MoS_2 (002) and MoS_2 (100) diffraction peaks appeared at Bragg angle 2θ= 14.38° and 32.7°， which indicates that the preferential growth of films on both lubricating surface and non-lubricated surface exist at the same time. MoS_2 peak intensity ratio I (100) / (I (002) + I (100)) was 0.24.

2) For MoS_2+Ti composite films, the intensity of both MoS_2 (002) and MoS_2 (100) diffraction peaks decreased, however, the (100) peak intensity MoS_2 reduced even more apparently. Peak intensity ratio I (100) / (I (002) + I (100)) dropped to 0.21, which shows the fact that the Ti atoms have more inhibition effect on the preferential growth of MoS_2 (100) on non-lubricated surface.

3) For MoS_2+Ti+C composite films, the preferential growth of MoS_2 (100) on non-lubricated surface was almost completely inhibited.

4) Based on the Scherrer equation [15-17], the average crystallite size of three kinds of films can be obtained: MoS_2-Ti-C ~ 5nm, MoS_2-Ti ~ 12nm, MoS_2 ~ 23nm. The reduction of crystallite size is conducive to increasing the film hardness.

4. Tribological behavior

4.1 Friction and wear tests

To evaluate the lubrication performance and longevity of different films, friction tests were performed using pin-on-disk device under EAST-like high vacuum and temperature condition. The friction coefficient curves were obtained and shown in Fig.7. All of the films have low friction coefficients at the beginning of tests, especially for MoS_2-Ti-C composite films (below 0.05). However, as the tests continued, the fluctuations increased. Finally, the pure MoS_2 films and composite MoS_2-Ti films sharply increased to more than 0.2 respectively at 150 min and 240 min, which indicates the coating films have already failed. The MoS_2-Ti-C composite films had a relatively stable friction performance throughout the whole 300 min test. Considering the testing parameters (rotation radius: 3mm, velocity: 1000rpm), it was roughly equivalent to 5600 meters of sliding distance.

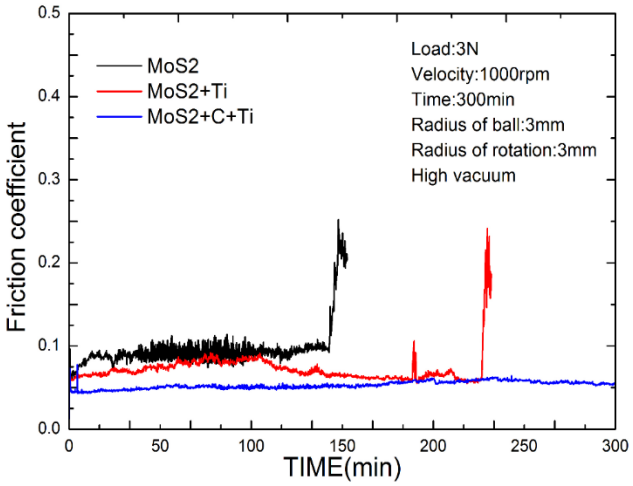

Fig. 7. The results of pin-on-disk test for different MoS2-based films

4.2 Scratch test

Scratch test is mainly used to study mechanical properties of thin coating films [18, 19]. As can be seen in Fig. 8, the curves for wear scars of three MoS2-based films were measured from scratch tests. The pure MoS_2 films were seriously worn with a scars of 500 μm wide and 4.1 μm deep. The curve for MoS_2+Ti the scars of 480μm wide and 2.8μm deep, did not improved a lot. For MoS_2+C+Ti films, both the width and deepth of wear scars have a significant reduction to 250μm and 0.8μm, decreasing a magnitude of its cross section. This shows MoS_2+C+Ti composite films have the highest surface hardness and wear resistance.

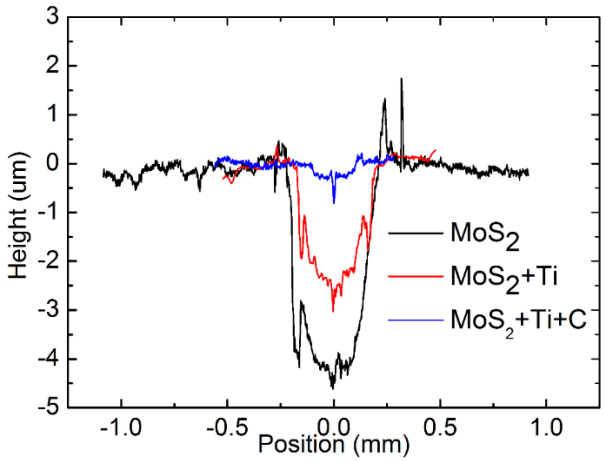

Fig. 8. The curves for wear scars of three MoS2-based films measured from scratch test

5. Summary

In this paper, three kinds of MoS2-based films were developed using multi-target magnetron sputtering deposition technique to find a suitable solution of solid lubrication for EAMA robot.

1) The SEM images and XRD patterns shown that the crystallites of composite thin films have finer size and more compact microstructure than pure MoS_2. The average crystallite size of MoS_2+C+Ti is around 5nm, much smaller than MoS_2 of 23nm.

2) Pin-on-disk tests directly demonstrated the higher performance of MoS_2+C+Ti composite films for both friction coefficient (below 0.05) and longevity (more than 300000 cycles).

3) Scratch tests also indicated the fact that MoS_2+C+Ti films have the relatively highest surface hardness and wear resistance.

Finally, MoS_2+C+Ti composite films have been supposed to be the most suitable selection for EAMA robot's lubrication under high vacuum and temperature. The coatings have been applied on the bearings and gears exposed to vacumm (shown in Fig.9). The implentation inside the EAST tokamak (Fig.10) shown a good performance of solid lubricating and protecting vacuum condition. Further tests have been finished to characteriticed the detailed information (listed in Table 2) for the solid lubricating products which can provide some references for similar applications.

Fig. 9. The bearings and gears after coating MoS_2 thin films

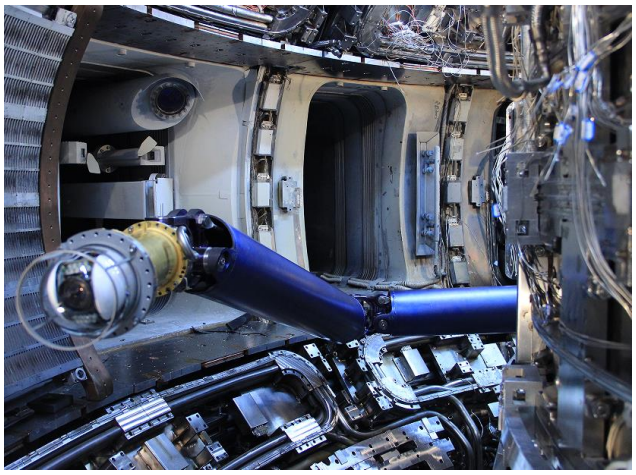

Fig. 10. The implentation of EAMA robot with solid lubrication

Table. 2. Specifications of MoS_2-Ti-C composite thin films

Testing items	Measured valves
film adhesion strength	30N
Friction coefficient	≤0.05 (high vacuum)
	≤0.09 (dry air)
	≤0.13 (80% humidity)
Wear rate	7.2×10^{-7} mm^3/Nm
Wear lifetime	≥320000 cycles
Load capacity	≥1.0GPa

References

[1] Yuanxi W, Jiangang L, Peide W. First engineering commissioning of EAST tokamak [J]. Plasma Science and Technology, 2006, 8(3): 253.

[2] Wu S, EAST Team. An overview of the EAST project [J]. Fusion Engineering and Design, 2007, 82(5): 463-471.

[3] Wan B, Li J, Wu Y. Progress in technology and experiment of superconducting tokamaks in ASIPP [J]. Fusion Engineering and Design, 2010, 85(7): 1048-1053.

[4] Luo G N, Zhang X D, Yao D M, et al. Overview of plasma-facing materials and components for EAST [J]. Physica Scripta, 2007, 2007(T128): 1.

[5] Song Y T, Peng X B, Xie H, et al. Plasma facing components of EAST[J]. Fusion Engineering and Design, 2010, 85(10): 2323-2327.

[6] Shi S S, Song Y T, Cheng Y, et al. Design and Implementation of Storage Cask System for EAST Articulated Inspection Arm (AIA) Robot[J]. Journal of Fusion Energy, 2015, 34(4): 711-716.

[7] Shi S, Song Y, Cheng Y, et al. Conceptual design main progress of EAST Articulated Maintenance Arm (EAMA) system [J]. Fusion Engineering and Design, 2016, 104: 40-45.

[8] Hathiramani D, Lingertat J, Van Eeten P, et al. Full-scale friction test on tilted sliding bearings for Wendelstein 7-X coils [J]. Fusion Engineering and Design, 2009, 84(2): 899-902.

[9] Koch F, Nocentini R, Heinemann B, et al. MoS 2 coatings for the narrow support elements of the W-7X nonplanar coils[J]. Fusion Engineering and Design, 2007, 82(5): 1614-1620.

[10] Aouadi S M, Paudel Y, Luster B, et al. Adaptive Mo2N/MoS2/Ag tribological nanocomposite coatings for aerospace applications[J]. Tribology Letters, 2008, 29(2): 95-103.

[11] Ye M, Zhang G, Ba Y, et al. Microstructure and tribological properties of MoS 2+ Zr composite coatings in high humidity environment[J]. Applied Surface Science, 2016.

[12] Wan Z H, Zhao Y P, Cai M M, et al. Wear process and analysis of lubrication failure about sputtering MoS2 composite solid films applied to spacecraft[C]//Applied Mechanics and Materials. Trans Tech Publications, 2013, 275: 1671-1677.

[13] Wang D Y, Chang C L, Chen Z Y, et al. Microstructural and tribological characterization of MoS 2–Ti composite solid lubricating films [J]. Surface and Coatings Technology, 1999, 120: 629-635.

[14] Wang D Y, Chang C L, Ho W Y. Microstructure analysis of MoS2 deposited on diamond-like carbon films for wear improvement [J]. Surface and Coatings Technology, 1999, 111(2): 123-127.

[15] Jiang H G, Rühle M, Lavernia E J. On the applicability of the x-ray diffraction line profile analysis in extracting grain size and microstrain in nanocrystalline materials [J]. Journal of materials research, 1999, 14(02): 549-559.

[16] Drits V, Srodon J, Eberl D D. XRD measurement of mean crystallite thickness of illite and illite/smectite: Reappraisal of the Kubler index and the Scherrer equation [J]. Clays and clay minerals, 1997, 45(3): 461-475.

[17] Monshi A, Foroughi M R, Monshi M R. Modified Scherrer equation to estimate more accurately nano-crystallite size using XRD [J]. World Journal of Nano Science and Engineering, 2012, 2(03): 154.

[18] Bull S J. Failure mode maps in the thin film scratch adhesion test [J]. Tribology International, 1997, 30(7): 491-498.

[19] Akono A T, Ulm F J. An improved technique for characterizing the fracture toughness via scratch test experiments [J]. Wear, 2014, 313(1): 117-124.